Pages: 35-44 / Vol. 18 / Issue 2 / Summer-Fall 2025

Journal of Aerospace Science and Technology

Journal Homepage: https://jast.ias.ir

Original Research Article

Calibration of Empirical Coefficients in Wake-Oscillator Model for Vortex-Induced Vibrations Using Genetic Algorithms

Farzaneh Hariri Akbari[1], Amin Taraghi Osguei[2*], Mehrdad Morovatdel[3], and Amir Kiyoumarsioskouei[4]

1, 2, 3, 4. Faculty of Mechanical Engineering, Sahand University of Technology, Tabriz, Iran
2, 4. Institute of Applied Energy, Sahand University of Technology, Tabriz, Iran

TICLE INFO

Received: 05 August 2024
Revised: 07 December 2024
Accepted: 08 January 2025
Available online: 12 April 2025

KEYWORDS:

Wake-oscillator model
Vortex-induced vibration
Genetic algorithm
Root mean square

ABSTRACT

Vortex-Induced Vibrations (VIV) occur when fluid flows around an object and generates oscillatory motion. In particular, fluid flow around a cylinder forms a symmetric vortex street pattern leading to VIV. This study employs a mathematical wake-oscillator model to simulate the VIV phenomenon. To refine the model, the genetic algorithm is utilized to determine the empirical coefficients of the mathematical model. An optimization approach is utilized for improved calibration of the model's prediction with experimental data, which integrates the Root Mean Square (RMS) objective function with the weighted contribution of the points. The results reveal that the empirical coefficients defined through the genetic algorithm maintain the quality of the super-upper branch prediction and present a better prediction for experimental observations. However, further steps are required to properly select empirical coefficients in wake oscillator models. The utilization of hybrid functions by combining multiple metrics can be one of the suitable choices.

DOI:
https://doi.org/10.22034/jast.2025.471867.1202

1 INTRODUCTION*

VIV occurs when a slender structure interacts with a fluid flow, causing oscillatory motion. These vibrations are a specific category of flow-induced vibrations, studied through the principles of fluid dynamics and structural mechanics [1]. This phenomenon is observed in marine structures such as risers and pipelines, which is one of the main causes of fatigue damage [2]. In recent years, this approach has progressed significantly and is now applied to both two-dimensional (2D) and three-dimensional (3D) vibrations [3,4]. The interaction between fluid and structure is a fascinating and contentious topic among engineers. When fluid flows over a solid body, flow separation occurs, forming a vortex street behind the body. The flow separation creates vortices which shed into the flow and lead to Von Kármán vortex street [5,6]. Among the studies conducted in the field of flow-induced vibrations, the flow over a cylinder is one of the classical structures compared to the flow-induced vibration of other structures. The simplicity of this model has increased its application in various studies, including the use in

* Corresponding Author's Email: taraghi@sut.ac.ir

Print ISSN:1735-2134 Online ISSN: 2345-3648

offshore facilities, power transmission lines, industrial chimneys, and more [7]. Due to its high computational speed, the wake oscillator model is one of the most commonly used semi-empirical models for predicting VIV responses [8].

From 1972 to 1979, practical concepts related to flow-induced vibrations and their applications were introduced in various industries, including mechanical mechanisms, civil structures, aerospace structures, shipbuilding, and nuclear power plants. Additionally, in the field of VIV, new and impactful topics relevant to industries and structures are emerging that can be studied and investigated by researchers [3]. Many researchers have conducted valuable studies on the behaviour of cylinders oscillating under VIV and the changes in lift and drag forces acting on the cylinder. The classification of these studies can be divided into numerical simulations with a single degree of freedom, two degrees of freedom models, and experimental tests.

Single-degree-of-freedom models are commonly employed in the study of VIV for cylinders exposed to fluid flow. These models are primarily considered as a mass-spring-damper system. Numerous models have been proposed to investigate vibrations with a single degree of freedom, and several models have provided the foundations for further research and studies. Bearman [9] investigated the VIV and related models by exposing a cylinder to fluid flow and linking the flow separation to the Reynolds number and the boundary layer formed on the body. The Reynolds number that causes the vortices to form behind the body is called the critical Reynolds number. Facchinetti et al. [10] studied VIV using a single degree of freedom model by coupling this model with displacement, velocity, and acceleration. They claimed that the best coupling occurs with the acceleration of a moving cylinder. Michel Dahl [11] widely worked on VIV, providing explanations for both single-degree-of-freedom and two-degree-of-freedom vibration models. Mahmoud et al. [12] used classical model equations for a single-degree-of-freedom cylinder to enhance energy generation from a piezoelectric device. Their time-based simulations demonstrated the coherence among the cylinder, piezoelectric device, and flow. The study highlighted that the interaction between the electrical and mechanical components can improve the design and efficiency of energy harvesting from VIV. Chen and Zhou [13] studied a single degree of freedom model for a cylinder placed in uniform fluid flow. Their research demonstrated that the proposed aerodynamic model effectively shows VIV's lock-in range and amplitude. The lock-in phenomenon happens when the vortex shedding frequency becomes close to the fundamental natural frequency of a vibrating structure. Synchronization of oscillation frequency and shedding frequency in a range of frequencies near the natural frequency can be characterized by a high amplitude of structural vibration, leading to fatigue or failure of structures. Bishop and Hassan [14] introduced the concept of the wake-oscillator equation by incorporating nonlinear Rayleigh and Van der Pol equations in their coupled wake-oscillator models. Zhang et al. [15] investigated a flexible structure and derived equations highlighting nonlinear parameters. Their research focused on enhancing VIV performance control through the use of a nonlinear energy sink. Liao et al. [16] numerically investigated the Fluid-Structure Interaction (FSI) on a cylinder in the upstream flow with a 2m/sec velocity. Their results indicated that the aspect ratio in the downstream plays a significant role in regulating the cylinder vibration. Fareshidianfar et al. [17] introduced a modified classical wake-oscillator model to investigate the vibration of the cylinder in the lock-in area. The response obtained through their model predicts the experimental results better than previous models, showing a reduced lock-in range and lower maximum oscillation amplitude on a Griffiths scope diagram. Zhao [18] investigated flow control of VIV in cylinders using techniques such as slotted plates, control rods, riblets, and rough surfaces. The study concluded that riblets and helical grooves provide the most effective suppression. Stansby [19] investigated the VIV in the context of single-degree-of-freedom cylinders. The studies are focused on the oscillations that occur in a direction perpendicular to the flow, arising from the wake vortices generated around the cylinder. Xu et al. [20] modified the classical wake oscillator model by refitting the empirical coefficient to make the wake oscillator model more accurate. Landl [21] developed a novel model to capture the hysteresis effect observed in experimental data on transverse vibrations. This consideration of the hysteresis phenomenon is particularly significant for conditions with a mass ratio below six.

In the prediction and analysis of VIV, single-degree-of-freedom models are commonly used.

However, in reality, in-line (parallel to flow) and cross-flow (perpendicular to flow) motions occur simultaneously, indicating the two degrees of freedom models [22]. Nayfeh et al. [23] studied the lift and drag forces on a circular cylinder using van der Pol and Rayleigh equations. Qu and Metrikine [24] improved a wake oscillator model by introducing a nonlinear wake variable to describe in-line motion. This enhancement was designed to increase the model's accuracy, particularly in cases with low mass ratios.

The complexity of VIV often encourages researchers to rely on simulation software tools when seeking to solve associated problems. In this regard, Stringer et al. [25] employed ANSYS and Open FOAM software to compute the flow around a cylinder. They considered a wide range of diameters and flow conditions for Reynolds numbers ranging from 40 to 106. Hasanpour et al. [26] investigated the impact of instabilities induced by vortices on the fluid flow dynamics around a cylinder and analysed its response.

This work follows on from and completes two earlier studies by the team that dealt with the simulation and experimental investigation of vortex-induced vibrations [27,28]. In fact, this research aims to optimize an objective function for determining the empirical coefficients of the wake-oscillator model using the proposed genetic algorithm. The optimization aims to improve the accuracy of the model's frequency response, enhancing its ability to accurately predict experimental results. Therefore, this paper is organized as follows. In the second section, a laboratory setup is constructed as an experimental oscillator, and the experimental results are obtained. In the third section, the mathematical model of the wake-oscillator is described, and the numerical results of this model are depicted in section four and optimized using a genetic algorithm and the proposed objective function. In the final section, the experimental and mathematical model results are compared to evaluate the performance of the selected objective function.

2 EXPERIMENTAL SETUP

Performing experimental investigations in VIV is a crucial approach for enhancing our understanding of the dynamic behavior exhibited by structures when subjected to fluid flow. In this section, a laboratory setup incorporating a wind tunnel is utilized to simulate and measure the displacement of a cylinder subjected to VIV. The frame is constructed using metal tubes with dimensions of 20×20 mm and a thickness of 2 mm. In order to improve the stability of the system and reduce vibrations resulting from the structure's placement within the wind tunnel, metal bars fabricated from CK45 steel are employed. The bars are mounted at the lower part of the structure to support the main structure, which is illustrated in Figure 1 (b).

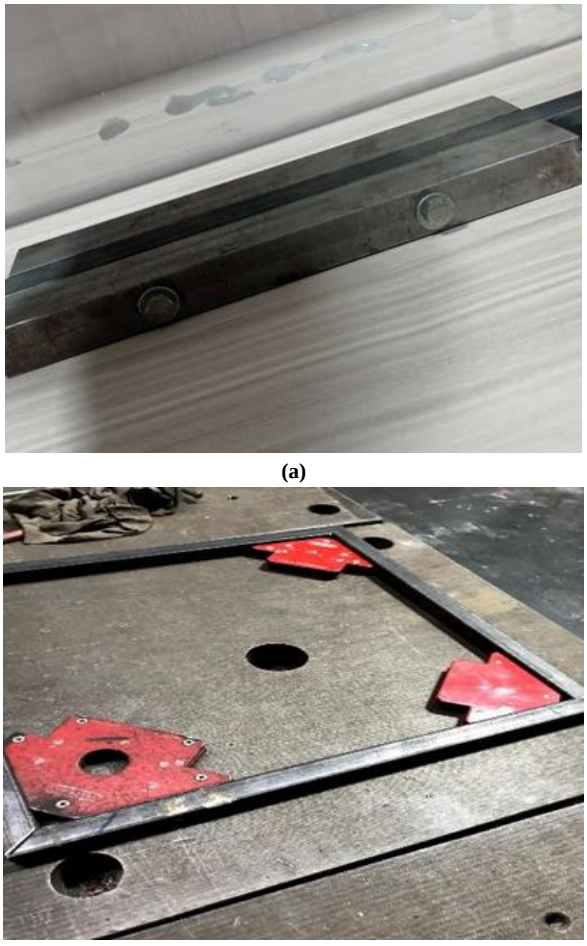

(a)

(b)

Fig 1. The experimental setup: (a) Frame of the main structure, **(b) Supporting metal bars**

For the suspension mechanism of the system, two metal sheets with dimensions of 40mm × 300mm and a thickness of 1mm are utilized. As illustrated in Figure 2 (a), a shaft is installed to support the cylinder, ensuring its correct positioning at the middle of the structure. For this setup, a cylinder with a diameter of 160mm and a length of 230mm is utilized. It weighs 40 grams and is fabricated

from compressed foam, as shown in Figure 2 (b). To establish a smooth surface, a thin layer of nylon is applied. A ruler with an indicator is used to measure the displacement of the cylinder and the impact of fluid flow. Additionally, a camera capable of capturing 240 to 960 frames per second is used to record and store the data.

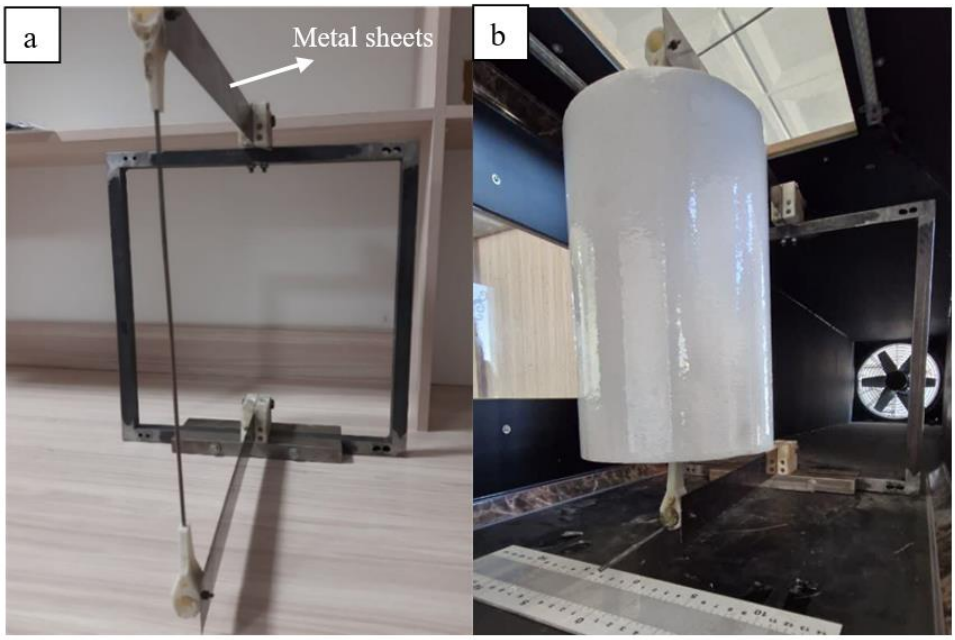

Fig 2. (a) The main structure of the setup with the metal sheet springs, (b) The experimental setup with a cylindrical bluff body with a diameter of 160mm

The wind tunnel utilized for conducting the experiment is located at the Faculty of Mechanical Engineering at Sahand University of Technology in Tabriz, with a length of 4 meters as depicted in Figure 3. The diffuser incorporated in the tunnel features an inlet with dimensions of 2.96 × 0.8 × 0.8m. Additionally, the nozzle installed for the flow entry is 1.4 × 1.4 × 0.45m. The wind tunnel is equipped with a three-phase fan with a diameter of 0.725 meters to generate the airflow. During the experiment, the wind tunnel is capable of producing velocities ranging from a minimum of 0.67 m/s up to a maximum of 8 m/s. These specific velocities are utilized to simulate different flow conditions affecting the cylinder and measuring its displacement accordingly.

Fig 3. Different views of the wind tunnel: (a) Up view, (b) Left view

Figure 4 illustrates the relationship between the amplitude of vibration and fluid velocity. The graph shows how the system's oscillation amplitude varies with different velocities corresponding to its oscillation frequency. The experimental data have been used to obtain the maximum dimensionless amplitude ($A^* = A_{max}/D$) of the cylinder with respect to the dimensionless reduced velocity ($U^* = 2\pi U/(\omega_s D)$).

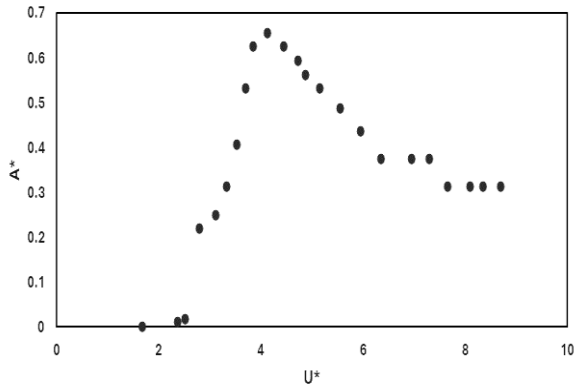

Fig 4. The variation of maximum amplitude response according to reduced velocity for the experimental setup

According to Figure 4, the system reaches its maximum oscillation amplitude at a fluid velocity of 1.65 m/s. At this point, the reduced dimensionless velocity is 4.125, which corresponds to the maximum peak dimensionless amplitude. This behavior can be attributed to the system's natural frequency being close to the vortex shedding frequency, leading to resonance and the resulting amplification of the oscillation amplitude.

2.1 Wake-Oscillator Model

In order to analyse the vibrational behavior of a cylinder caused by VIV, it is essential to select an appropriate wake-oscillator model that comprehensively captures all aspects associated with the cylinder's vibrations. These mathematical models accurately represent vibrations resulting from the interaction between the structure and the fluid ambiance. These models typically employ differential equations that incorporate empirical coefficients and experimental data, allowing for the simulation and analysis of VIV in the cylinder. By utilizing these mathematical models, it becomes feasible to accurately simulate and analyse the dynamic behavior of the cylinder subjected to VIV. The specific form of the wake-oscillator model will depend on the characteristics of the system and the desired level of accuracy in the analysis. These models can be modified and calibrated through the optimization of empirical coefficients [18].

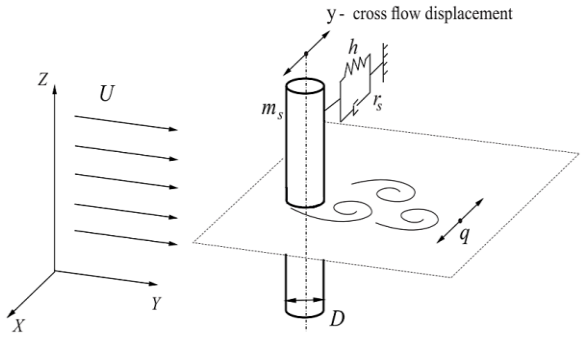

Fig 5. A one-degree-of-freedom model for a cylinder capable of vibrating perpendicular to the flow direction [3]

The vibrational behavior of the system can be described by a pair of coupled equations: one represents the displacement of the cylinder, while the other captures the strength of the wake (vortex street) generated behind the cylinder. The wake is modelled using the Van der Pol equation, a well-known nonlinear differential equation commonly employed to describe oscillatory systems, particularly those characterized by self-sustaining oscillations. Figure 5 provides a visual representation of the setup, illustrating a cylinder of diameter D surrounded by a fluid flow with velocity U. The cylinder remains stationary in the direction of the flow but exhibits motion perpendicular to the flow direction. Figure 5 depicts the model utilized in this study to study the cylinder's behavior with one degree of freedom.

The cylinder with diameter D is affected by the flow with velocity U, and oscillates transversely. Therefore, it is possible to express the motion of the cylinder as follows [8]:

$$m\ddot{y} + r\dot{y} + ky = S \tag{1}$$

$$S = \frac{1}{2}\rho U^2 D C_l \tag{2}$$

where y, k, S, ρ, and U are the transverse displacement of the cylinder, stiffness of the spring, fluid force, fluid density, and fluid velocity. Additionally, D and C_l are the diameter of the oscillating cylinder and the lift force coefficient, respectively. In addition, r and m are the total damping and mass of the system that can be defined as:

$$m = m_s + m_f$$
$$r = r_s + r_f \quad (3)$$

In the above equations, r_s and m_s are the damping and mass of the cylinder, while r_f and m_f are the added damping and mass of the system. These two parameters can be defined as follows:

$$m_f = \frac{\pi C_m \rho D^2}{4}$$
$$r_f = \gamma \omega_s \rho D^2 \quad (4)$$

In relation (4), C_m, γ, and ω_s are the added mass coefficient, fluid-added damping coefficient, and the angular frequency of cylinder vibration that relates to the fluid velocity (U), Strouhal number (St), and the diameter of the cylinder (D) as shown in equation below:

$$\omega_s = \frac{2\pi StU}{D} \quad (5)$$

The final equations of the wake-oscillator model are derived by combining the equations of motion and the Van der Pol equation, incorporating relevant simplifications. The resulting equations can be expressed as follows [18]:

$$\ddot{y} + (2\xi\delta + \frac{\gamma}{\mu})\dot{y} + \delta^2 y = Mq \quad (6)$$

$$\ddot{q} + \varepsilon(q^2 - 1)\dot{q} + q = N\ddot{y} \quad (7)$$

In these equations, the empirical coefficients ε and N play a crucial role in this model. Determining the most suitable values for these coefficients is the primary objective of this research. Additionally, the constant coefficient M is calculated using the following equation:

$$M = \frac{C_{l0}}{4\pi^3 St^2 \mu} \quad (8)$$

The parameter δ represents the ratio of the vortex shedding frequency to the natural frequency of the cylinder. It provides a quantitative representation of how the inherent vibration frequency of the cylinder relates to the frequency at which vortices are shed from the cylinder due to the fluid flow. In addition, ξ and μ are the damping ratio and the mass ratio, respectively.

3 RESULTS AND DISCUSSION

The wake-oscillator mathematical model incorporates two empirical coefficients that can be optimized for predicting experimental results. The calibration process involves optimizing the value of empirical coefficients ε and N to ensure that the wake-oscillator model can predict the observed experimental data. By fine-tuning these coefficients, the mathematical model more accurately captures the vibrational behavior of the system, thereby increasing its predictive capabilities increases. Two methods have been employed to estimate these coefficients with the objective of obtaining the optimal values. In the first method, the empirical coefficients are manually adjusted within various intervals, and the results for three examples are illustrated in Figure 6. Through multiple trial-and-error iterations, the range of 5 to 15 for N and 0.01 to 0.9 for ε has been determined as the most suitable selection for the empirical coefficients based on the obtained outcomes. To determine the most optimal solution, a weighted RMS objective function has been utilized, aiming to minimize the differences between experimental data and the results of the model. By minimizing these differences, the weighted RMS objective function provides the best approximation and a good agreement between the mathematical model and the experimental data.

Figure 6 illustrates the results of the model for three different pairs of coefficients through the mathematical model. The first one with N=8 and ε=0.03, the results of the model fall within the specified range; however, in the second curve, with N=3 and ε=0.2, N is outside the specified range while ε remains within it. The third case represents the prediction of the model when both empirical coefficients are outside the specified range. It is evident that there is a significant difference between the results obtained for the coefficients outside the selected range and the experimental results. Conversely, the results obtained using values within the selected range (N and ε) have a superior prediction with the experimental data compared to the other cases. Additionally, upon examining the numerical results derived from the objective function, it is clear that the graph wherein both empirical coefficients fall within the specified range exhibits the lowest error value compared to the other cases.

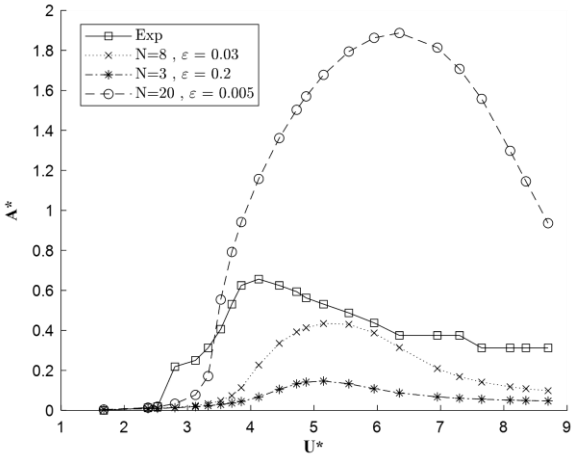

Fig 6. A one-degree-of-freedom model with different empirical coefficients

Subsequently, Table 1 presents the results of the RMS objective function that were obtained. According to Table 1, the graph corresponding to the empirical coefficients through the specified range exhibits the lowest value for the objective function. The results indicate that the corresponding graph provides the most optimal and closest response, among these three cases, to the experimental data. Further minimization of the objective function reinforces the superior calibration of the results with the experimental data.

Table 1. Various values selected for empirical coefficients

#	N	ε	RMS
1	8	0.03	0.241
2	3	0.2	0.369
3	20	0.005	0723

As mentioned, at the first step, the trial-and-error approach was used to find suitable intervals for the empirical coefficients by evaluating different values. However, manually finding the best values that result in the lowest error can be a time-consuming and impossible process. To overcome this problem, in the second step, the genetic algorithm has been utilized to determine the optimal values for the empirical coefficients. The genetic algorithm is a search heuristic inspired by the process of natural selection. It involves creating a population of potential solutions and iteratively evolving them to find the best solution. By using the genetic algorithm, the search space for the empirical coefficients can be efficiently explored, leading to the identification of values that minimize the error. This automated approach saves time and improves the accuracy of the estimation process for coefficients.

To enhance the optimization process, a genetic algorithm is employed, incorporating the RMS objective function along with a weighted contribution of points. For each empirical coefficient, an appropriate range is selected as input for the genetic algorithm. To further enhance the prediction accuracy of the model, a weighting pattern is applied to the objective function points. This pattern, as illustrated in Table 2, assigns higher weights for peak points and progressively reduces the weight for other points to maintain the quality of the super-upper branch prediction.

Table 2. Weighting coefficients used in the optimization process.

Points	1	2	3	4	5	6	7	8	9	10	11	12	13	14	15	16	17	18	19	20	21	22	23
Weight	0	2	0	1	0	1	0	1	0	3	4	0	0	2	0	1	0	1	0	1	0	1	0

The algorithm utilizes the specified ranges to construct different pairs of coefficients, to initiate the search for the optimal values of N and ε. The genetic algorithm determines values for N and ε and utilizes them for optimization based on the RMS function. The pair of values that yields the lowest RMS value represents the optimal solution for the wake-oscillator mathematical model. The range for ε is selected between 0.01 to 0.9, while N varies from 5 to 15. These ranges provide suitable boundaries for the genetic algorithm to explore and identify the most effective values for the empirical coefficients N and ε in the wake-oscillator model.

The RMS objective function plays a crucial role in the calibration of a mathematical model with experimental data. The weighted RMS objective function facilitates improvement in defining the empirical coefficients of the model. One significant advantage of utilizing the RMS objective function is its ability to compute the value for each individual in the population. This individual-level evaluation provides a more comprehensive assessment of model performance.

$$RMS = \sqrt{\frac{1}{n}\sum_{i=1}^{n}[w_i(y_{\exp_i} - y_{num_i})]^2} \quad (9)$$

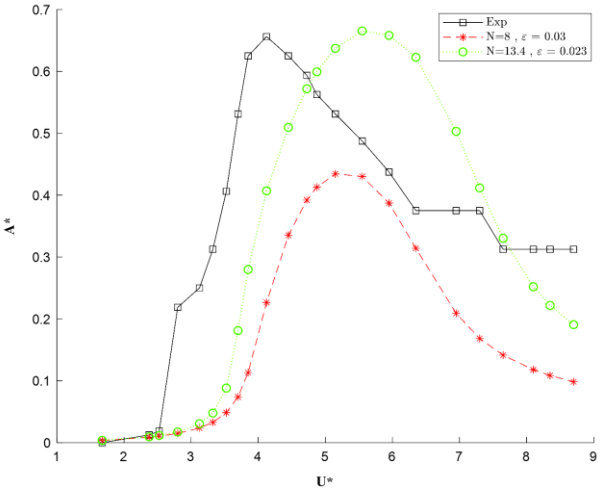

Fig 7. Maximum amplitude according to the reduced speed for the RMS objective function based on trial-and-error (N=8, ε=0.03) and genetic algorithm (N =13.44, ε =0.023).

For the investigated model, the values obtained for the empirical coefficients of N and ε from the genetic algorithm based on the RMS objective function are 13.44 and 0.023, respectively. Figure 7 illustrates the mathematical model prediction, highlighting the prioritization of peak points in the weighting scheme. The peak values receive greater emphasis compared to other points, resulting in improved compatibility between the mathematical model and experimental data. It is evident that the peak of the mathematical model exhibits a good prediction of the peak of the experimental data. As the distance from the peak increases, the compatibility of the points progressively diminishes. These findings highlight the effectiveness of the genetic algorithm, weighted RMS objective function, and point weighting algorithm in refining the mathematical model and enhancing its predictive capabilities. The optimized values of coefficients and the weighting approach contribute to a more accurate representation of the system dynamics, facilitating improved model performance and close fitting with experimental observations.

4 CONCLUSION

The aim of this research is to enhance the calibration of the mathematical wake-oscillator model with experimental data. The experimental results are collected for a developed laboratory setup using a wind tunnel. The obtained results are used to define the empirical coefficients of the mathematical model through the genetic algorithm, by employing the RMS with weighted contribution of the points as an objective function. The integration of the weighting algorithm with the RMS objective function significantly improved the accuracy of the wake-oscillator model. The findings underscore the effectiveness of the conventional RMS objective function in optimizing model coefficients. For future studies, other objective functions such as peak height or hybrid functions combining multiple metrics will be explored. These alternatives could provide further insights into the model's behavior and enhance precision by addressing specific aspects of the calibration of the mathematical model and experimental results.

CONFLICT OF INTEREST

No potential conflict of interest was reported by the authors.

REFERENCES

[1] V. Kurushina, E. Pavlovskaia, A. Postnikov, and M. Wiercigroch, "Calibration and comparison of VIV wake oscillator models for low mass ratio structures," *Int. J. Mech. Sci.*, vol. 142–143, pp. 547–560, 2018, https://doi.org/10.1016/j.ijmecsci.2018.04.027

[2] V. Kurushina and E. Pavlovskaia, "Fluid nonlinearities effect on wake oscillator model performance," *MATEC Web Conf.*, vol. 148, pp. 4–9, 2018, https://doi.org/10.1051/matecconf/201814804002.

[3] A. Postnikov, E. Pavlovskaia, and M. Wiercigroch, "2DOF CFD Calibrated Wake Oscillator Model to Investigate Vortex-Induced Vibrations," *Int. J. Mech. Sci.*, vol. 127, pp. 176-190, 2017, https://doi.org/10.1016/j.ijmecsci.2016.05.019.

[4] H. Zanganeh and N. Srinil, "Three-dimensional VIV prediction model for a long flexible cylinder with axial dynamics and mean drag magnifications," *J. Fluids Struct.*, vol. 66, pp. 127–146, 2016, https://doi.org/10.1016/j.jfluidstructs.2016.07.004

[5] A. A. Shittu and F. Kara, "Review of offshore pipeline span creation mechanism," *Int. J. Res. Eng. Appl. Sci*., vol. 8, no. 2, pp. 31–53, 2018.

[6] M. M. Shabani, A. Taheri, and M. Daghigh, "Reliability assessment of free spanning subsea pipeline," *Thin-Walled Struct.*, vol. 120, pp. 116–123, 2017, https://doi.org/10.1016/j.tws.2017.08.026

[7] J. V. Ulveseter, M. J. Thorsen, S. Sævik, and C. M. Larsen, "Time domain simulation of riser VIV in current and irregular waves," *Mar. Struct.*, vol. 60, pp. 241–260, 2018, https://doi.org/10.1016/j.marstruc.2018.04.001.

[8] X.Zhang, X. Zhang, S. Zhou, W. Yang, L. Xu, L.Yi, G.Tian, Y. Ma, Y. Hao, and W. Ni, "A Modified Wake Oscillator Model for the Cross-Flow Vortex-Induced Vibration of Rigid Cylinders with Low Mass and Damping Ratios," *J. Mar. Sci. Eng.*, vol. 11, no. 2, 2023, https://doi.org/10.3390/jmse11020235.

[9] Bearman, Peter W, "Vortex shedding from oscillation bluff bodies," *Annual Review of Fluid Mechanics*, vol. 50, pp. 129–138, 1993, https://doi.org/10.1146/annurev.fl.16.010184.001211.

[10] M. L. Facchinetti, E. de Langre, and F. Biolley, "Coupling of structure and wake oscillators in vortex-induced vibrations," *J. Fluids Struct.*, vol. 19, no. 2, pp. 123–140, 2004, https://doi.org/10.1016/j.jfluidstructs.2003.12.004.

[11] J. M. Dahl, "Vortex-Induced Vibration of a Circular Cylinder with Combined In-line and Cross-flow Motion," Thesis PhD, Massachusetts Inst. Technol., pp. 1–26, 2008.

[12] A. Mehmood, A. Abdelkefi, M.R. Hajj, A.H. Nayfeh, I. Akhtar, A.O. Nuhait, "Piezoelectric energy harvesting from vortex-induced vibrations of circular cylinder," *Journal of Sound and Vibration*, vol. 332, no. 19, pp. 4656–4667, 2013, https://doi.org/10.1016/j.jsv.2013.03.033.

[13] W. L. Chen and F. Xu, "Investigation of a hybrid approach combining experimental tests and numerical simulations to study vortex-induced vibration in a circular cylinder," *J. Sound Vib.*, vol. 331, no. 5, pp. 1164–1182, 2012, https://doi.org/10.1016/j.jsv.2011.10.016.

[14] R. E. D. Bishop and A. Y. Hassan, "The lift and drag forces on a circular cylinder in a flowing fluid," Proc. R. Soc. London. Ser. A. Math. Phys. Sci., vol. 277, no. 1368, pp. 32–50, 1964, https://doi.org/10.1098/rspa.1964.0004.

[15] M. Zhang, T. Wu, and O. Øiseth, "Vortex-induced vibration control of a flexible circular cylinder using a nonlinear energy sink," *J. Wind Eng. Ind. Aerodyn.*, vol. 229, no. March 2022, https://doi.org/10.1016/j.jweia.2022.105163

[16] W. Liao, Z. Huang, H. Sun, X. Huan, Y. Gu, W. Chen, Z. Zhang, and J. Kan, "Numerical investigation of cylinder vortex-induced vibration with downstream plate for vibration suppression and energy harvesting," *Energy*, vol. 281, No. Article 128264, 2023, https://doi.org/10.1016/j.energy.2023.128264.

[17] A. Farshidianfar, N. Dolatabadi, and Y. Naranjani, "Consideration of Lock-in Using a Modified Wake Oscil- lator in Vortex Induced Vibrations about a Cylinder," *Iran. Soc. Acoust. Vib.*, pp. 1–7, 2011.

[18] M. Zhao, "A review of recent studies on the control of vortex-induced vibration of circular cylinders," Ocean Eng., vol. 285, p. 115389, 2023, https://doi.org/10.1016/j.oceaneng.2023.115389.

[19] P. K. Stansby, "The locking-on of vortex shedding due to the cross-stream vibration of circular cylinders in uniform and shear flows," *J. Fluid Mech.*, vol. 74, no. 4, pp. 641–665, 1976, https://doi.org/10.1017/S0022112076001985.

[20] W. H. Xu, Y. X. Wu, X. H. Zeng, X. F. Zhong, and J. X. Yu, "A new wake oscillator model for predicting vortex induced vibration of a circular cylinder," *J. Hydrodyn.*, vol. 22, no. 3, pp. 381–386, 2010, https://doi.org/10.1016/S1001-6058(09)60068-8.

[21] R. Landl, "A mathematical model for vortex-excited vibrations of bluff bodies," *J. Sound Vib.*, vol. 42, no. 2, pp. 219–234, 1975, https://doi.org/10.1016/0022-460X(75)90217-5.

[22] X. Bai and W. Qin, "Using vortex strength wake oscillator in modelling of vortex induced vibrations in two degrees of freedom," *Eur. J. Mech. B/Fluids*, vol. 48, pp. 165–173, 2014, https://doi.org/10.1016/j.euromechflu.2014.05.002.

[23] A. H. Nayfeh, F. Owis, M. R. Hajj "A model for the coupled lift and drag on a circular cylinder", *2003 ASME Design Engineering Technical Conferences and Computers and Information in Engineering Conference*, United States, Chicago, IL pp. 1289-1296. 2003,

[24] Y. Qu and A. V. Metrikine, "A single van der pol wake oscillator model for coupled cross-flow and in-line vortex-induced vibrations," *Ocean Eng.*, vol. 196, Att. no. 106732, 2020, https://doi.org/10.1016/j.oceaneng.2019.106732.

[25] R. M. Stringer, J. Zang, and A. J. Hillis, "Unsteady RANS computations of flow around a circular cylinder for a wide range of Reynolds numbers," Ocean Eng., vol. 87, pp. 1–9, 2014, https://doi.org/10.1016/j.oceaneng.2014.04.017.

[26] M. Hassanpour, C. Morton, and R. J. Martinuzzi, "Effect of harmonic inflow perturbation on the wake vortex dynamics of a cylinder undergoing two-degree-of-freedom vortex-induced vibration near a plane boundary," *Phys. Fluids*, vol. 34, no. 10, 2022, https://doi.org/10.1063/5.0115610.

[27] R. Mahmoodpoor, A. Kiyoumarsioskouei, A. Taraghi Osgue. "Experimental assessment of the air flow induced vibration of a single cylinder with a cantilever beam." *Journal of Aerospace Science and Technology*, 2024, https://doi.org/10.22034/jast.2024.445963.1178.

[28] A. Kiyoumarsioskouei, A. Taraghi Osguei. "Time and frequency analysis of fluctuating hydrodynamic forces acting on circular and square cylinders in laminar flows." *Journal of the Brazilian Society of Mechanical Sciences and Engineering* pp 45.6, 2023, https://doi.org/10.1007/s40430-023-04220-y.

HOW TO CITE THIS ARTICLE

F. Hariri Akbari, A. Taraghi Osguei, M. Morovatdel, and A. Kiyoumarsioskouei, "Calibration of Empirical Coefficients in Wake-Oscillator Model for Vortex-Induced Vibrations Using Genetic Algorithms," *Journal of Aerospace Science and Technology*, Vol. 18, Issue 2, 2025, pp. 35-44.

DOI: https://doi.org/10.22034/jast.2025.471867.1202

URL: https://jast.ias.ir/article_218676.html